Intelligent Automation And Soft Computing, 2019

Vol. 25, no. 4, 695–704
https://doi.org/10.31209/2019.100000073

Hybrid Modulation Strategy For Reactive Compensation Of PV Grid-Connected Inverter

Liao Tian-fa

School of Electronic information and Electronical Engineering, Huizhou University, Huizhou, Guangdong, 516007, China

ABSTRACT

With the spreading of Photovoltaic (PV) grid-connected system, grid-connected reactive-load compensation and harmonic control is becoming a research focus. Unipolar and bipolar modulations are widely used in active power filter of PV grid-connected inverter. Unipolar modulation is good at harmonic, ripples and efficiency control, while bipolar modulation is good at grid-connected current control. A comprehensive comparison between the aforementioned modulation strategies in aspects of basic switching action, effects on operation mode, current harmonics，efficiency, is done in this paper. Base on it, a hybrid modulation strategy with the fusion of the unipolar and bipolar modulation is proposed in this paper. Numerical and experimental results show the lowest total harmonic distortion, and enhanced zero passage control are achieved by the proposed method, providing a reliable and efficient control strategy for PV grid connecting.

KEYWORDS: Reactive Compensation; Unipolar modulation; Bipolar modulation; Hybrid modulation; PV grid-connected inverter

1 INTRODUCTION

THE thirst for new energy promotes the scale of photovoltaic grid-connected power generation to be expanded rapidly, and the influence of photovoltaic power generation on the power quality is also increasingly obvious. Moreover, our country faces the status quo of weak power grid structure, backward technological means of power transmission and distribution and low automation level. Hence, how to improve the voltage quality and govern harmonic has become one of the most urgent problems (Wang et al., 2017; Zhu et al., 2016; Ma et al., 2017; Liu et al.2017). At present, the study on the combination of photovoltaic power generation with reactive compensation of power grid and harmonic suppression has become a hotspot with the continuous advance of power electronic technology. Based on the rapid popularization of distributed power generation, the electric energy should be used effectively with a high quality as well as the reactive harmonic should be effectively and flexibly controlled so as to improve the voltage quality and lower the harmonic content(Xie et al.,2013; Zhao et al.,2018; Li et al., 2017).

Single-phase non-isolated photovoltaic grid-connected inverter was widely used in the photovoltaic grid-connected inverter system due to its small volume, light weight, high efficiency, and so on (Yi et al., 2015). Likewise, the inverter, which was the intermediate link between the solar arrays and power distribution system of alternating current, has an important role in the whole economic benefits of photovoltaic power generation system due to the factors such as security, reliability, inversion efficiency, manufacturing cost, and so on (Wang et al.,2013; Yuan et al.,2014; Xiao et al.,2014). Therefore, the high-quality inverter power supply has become an important research object of power supply technology.

The main circuit topology structure of the most commonly used photovoltaic grid-connected inverter is the full bridge inversion, as shown in Figure 1. The main circuit topology structure is composed of boost up circuit and full-bridge inverter circuit, and the post-stage full-bridge inverter circuit mainly converts the direct current to alternating current after the boost circuit.

CONTACT Liao Tian-fa liaotianfa123@163.com

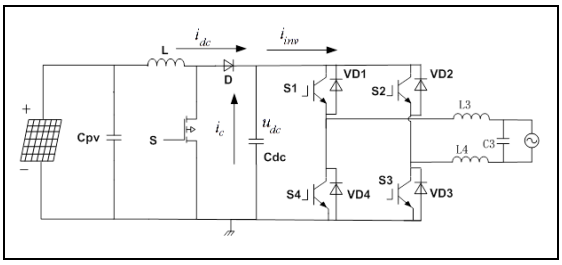

Figure.1 Main circuit topology of Single-phase Grid-connected PV Inverter

The solution of switch variables directly determines the output voltage of the inverter and then controls the amplitude and phase of the grid-connected output current. It is the last link for the system to carry out the active and reactive control as well as the most crucial link to affect the output power quality. In fact, the unipolar control and the bipolar control are widely used for the modulation of second-stage full-bridge inverter circuit. Furthermore, unipolar modulation has significant advantages in the harmonic wave, ripple wave, efficiency. However, there existed the zero-crossing distortion for current in the reactive power control circuit. This problem just can be solved by the bipolar modulation, but the bipolar modulation has the disadvantages, such as great switching loss, great electromagnetic interference, great switching harmonic, and so on. Therefore, hybrid modulation mode was put forward by the above two ways integration, and then the effectiveness and feasibility of this mode were verified by experiments.

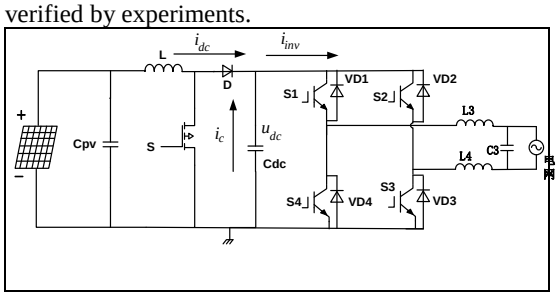

Figure.2 Main circuit topology of Single-phase Grid-connected PV Inverter

2 CONTRASTIVE ANALYSIS FOR UNIPOLAR MODULATION AND BIPOLAR MODULATION

THE waveform of unipolar and bipolar PWM control were shown in Figure 2. The modulating signal U_r was the sine wave. In the unipolar modulation, carrier U_t was the triangular wave with positive polarity in the positive half cycle of U_r, likewise, carrier U_t was the triangular wave with negative polarity in the negative half cycle of U_r. When using the bipolar modulation mode, the carrier U_t were both positive or negative in a half cycle of U_r. However, both kinds of modulation ways controlled opening and closing of IGBT at the time of intersections of U_r and U_t. Two kinds of modulation ways in Figure 2 are shown as follows (Kjaer et al., 2005):

Unipolar modulation:

When U_r is in the positive half-wave, S_1 is in an on-state, S_2 is in an off-state, S_4 is in an off-state. As $U_r > U_t$, S_3 is in an on-state, as $U_r<U_t$, S_3 is in an off-state.

When U_r is in negative half-wave, S_2 is in an on-state, S_1 is in an off-state, S_3 is in an off-state. As $U_r > U_t$, S_4 is in an off-state, as $U_r<U_t$, S_4 is in an on-state.

Bipolar modulation:

As $U_r>U_t$, S_1 and S_3 is in an on-state, as well as S_2 and S_4 is in an off-state. As $U_r<U_t$, S_2 and S_4 is in an on-state, as well as S_1 and S_3 is in an off-state.

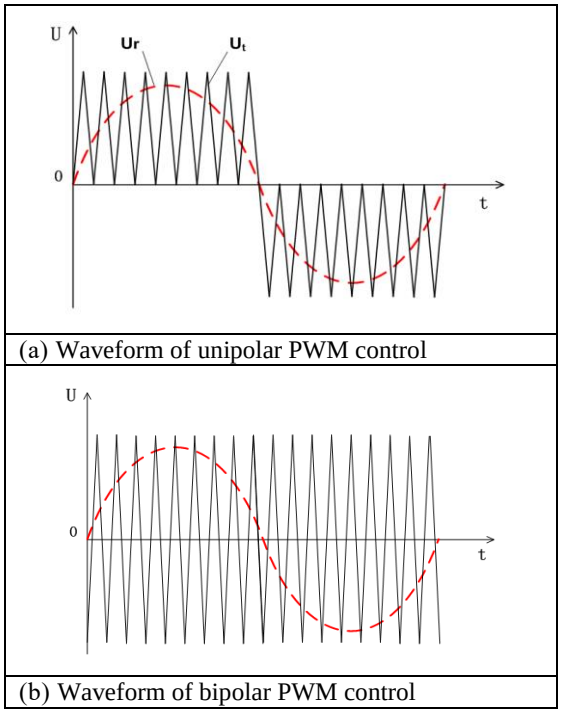

(a) Waveform of unipolar PWM control

(b) Waveform of bipolar PWM control

Figure.3 PWM control waveform

Obviously, four IGBT worked in a high-frequency on-off state under the bipolar modulation, thus resulting in more switching loss and higher EMI interference. Figure 3 shows the waveform of output voltage and inductive current of inverter under the two kinds of modulation modes.

As the unipolar modulation, the relationship between inductive current and output voltage of inverter was as follows.

$$L\frac{2\Delta i_{\max}}{DT_s} = U_{dc} - U_{av} \qquad (1)$$

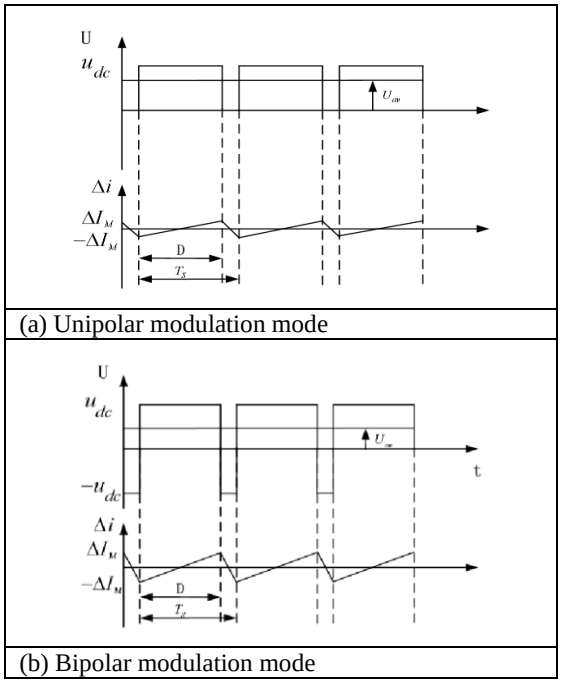

Figure.4 Output voltage and inductor current waveform of the inverter

$$i_{pp} = 2\Delta i_{\max} = \frac{(U_{dc} - U_{av})DT_s}{L} \tag{2}$$

Then the ripple current can be expressed as:

After passing through LCL filter circuit, the output voltage of inverter was:

$$e(\omega t) = \mu U_{dc} \sin(\omega t) \tag{3}$$

$$U_{av} = DU_{dc} \tag{4}$$

$$D = \mu \sin(\omega t) \tag{5}$$

where μ was modulation ratio. Let μ=0.8, and the formulas (3), (4) and (5) were substituted into formula (2), then:

$$\Delta i_{pp}(\omega t) = \frac{U_{dc}T_s}{L}(1 - \mu \sin(\omega t))\mu \sin(\omega t) \tag{6}$$

Similarly, the ripple current of bipolar modulation mode can be expressed as:

$$\Delta i_{pp}(\omega t) = \frac{U_{dc}T_s}{2L}(1 - \mu^2 \sin^2(\omega t)) \tag{7}$$

Figure 4 shows ripple current curve of both kinds of modulation modes in a range of 0 and π, and the ripple current amplitude has the same change tendency in the range of π and 2π as that in the range of 0 and π due to the half-wave symmetric feature of grid-connected current. It was observed that the ripple current amplitude of zero-crossing point by unipolar modulation was the smallest, but the ripple current amplitude of zero-crossing point by bipolar modulation was the largest.

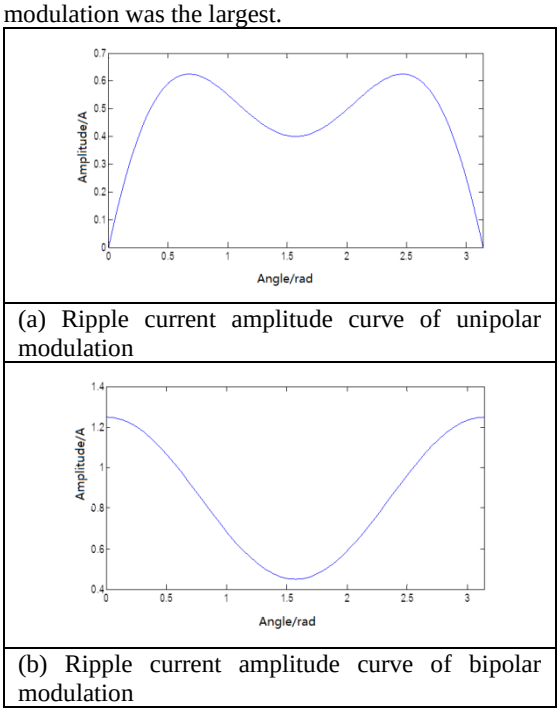

Figure.5 Amplitude curve of the ripple current

In half a period, the effective value of ripple current of unipolar modulation can be expressed as:

$$I_{rms} = \frac{U_{dc}T_s}{2L}\mu\sqrt{\frac{2}{3\pi}\left[\frac{\pi}{4}\left(1+\frac{3}{4}\mu^2\right)-\frac{4}{3}\mu\right]} \tag{8}$$

The effective value of ripple current of bipolar modulation can be expessed as:

$$I_{rms} = \frac{U_{dc}T_s}{4L}\sqrt{\frac{1}{3}\left(1-\mu^2+\frac{3}{8}\mu^4\right)} \tag{9}$$

where U_{dc} is 400V, T_S is 50μS, and L is 4mH. They are substituted into Equations (8) and (9), and thus obtaining the effective values of ripple current of unipolar modulation and bipolar modulation, 0.1425A and 0.2586A, respectively.

This paper constructed the simulation model of second-stage inverter circuit, as shown in Figure 5. In this model, the parameters in the DC side of inverter circuit are as follows. The voltage is set as 400Vdc, the command current is the sine AC with a amplitude of 15 A and a frequency of 50Hz. As well as the grid voltage is the sine AC with a amplitude of 310Vac and a frequency of 50Hz. The triangular carrier frequency is 20 Khz. The bipolar modulation is used,

and the value of each component of LCL filter circuit is 3mH, 2μF, and 3mH, respectively.

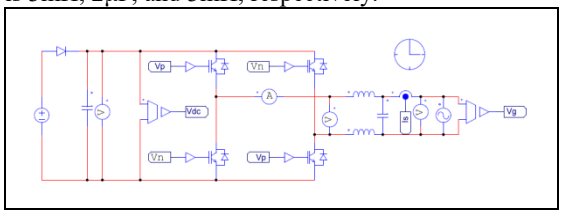

Figure 6. The simulation model of second-stage inverter circuit

By using the PSIM simulation model of the inverter circuit in Figure 5, when the amplitude of command current is 15A, the grid-connected current spectrograms of two modulation ways are obtained, as shown in Figure 6, as well as the total harmonic distortions of grid-connected current under different powers, listed in Table 1, are obtained.

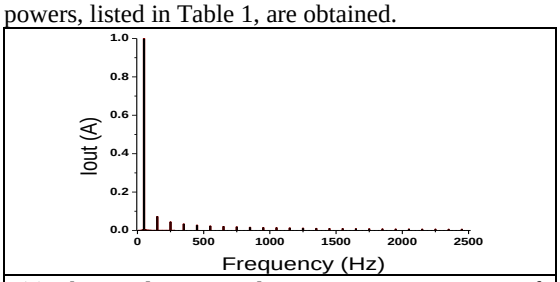

(a) the grid-connected current spectrograms of unipolar modulation

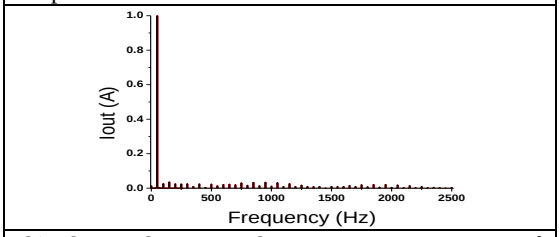

(b) the grid-connected current spectrograms of bipolar modulation

Figure 7 The grid-connected current spectrograms

Table 1 The total harmonic distortions of grid-connected current under different powers(THD%)

Instruction current amplitude(A)	THD of unipolar modulation	THD of bipolar modulation
2	14.55%	30.86%
4	7.21%	16.24%
8	3.58%	7.45%
12	2.40%	4.36%

It is known by analysis that the unipolar modulation is superior to the bipolar modulation in the efficiency, ripple, harmonic and so on. In the traditional photovoltaic grid-connected inverter, the same frequency and phase are needed for the grid-connected current, moreover, the grid-connected current of uniplar modulation should be distortionless at zero point. Hence, it is very suitable for the modulation of single-phase grid-connected inverter. However, as the grid-connected current phase is ahead of or lags behind that of the grid voltage, namely, the reactive output for grid-connected inverter, there would generate seriously distortion at zero point of power grid voltage, which greatly increases the total harmonic distortion rate(Chen et al.,2008; Manjili et al.,2013; Lasseter et al.,2010). For the same reactive power, the power quality is completely incompatible with the grid-connected requirement.

3 ANALYSIS FOR ZERO-CROSSING DISTORTION OF CURRENT BY UNIPOLAR MODULATION AND BIPOLAR MODULATION

FIGURE 7 (a) showed the unipolar driving waveform, and Figures (b) and (c) showed the waveforms of grid-connected current ahead of and lagging behind grid voltage when the unipolar modulation output reactive power.

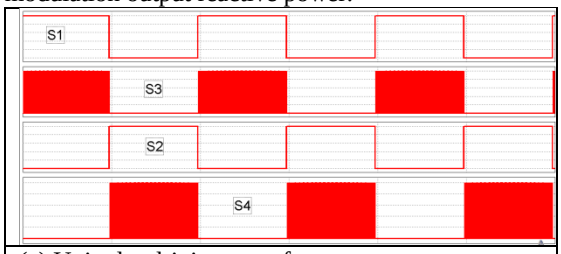

(a) Unipolar driving waveform

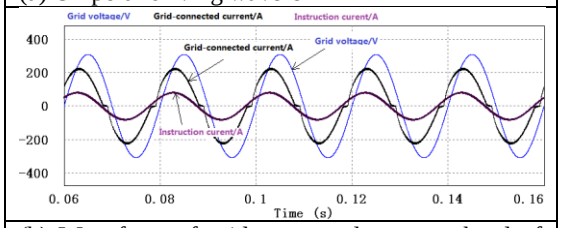

(b) Waveform of grid-connected current ahead of grid voltage

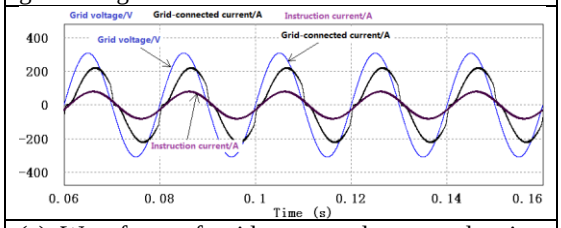

(c) Waveform of grid-connected current lagging behind grid voltage

Figure.8 Grid current and voltage waveform of the unipolar modulation

As shown in Figure 7, there is no zero-crossing distortion for the current, which suggests that the solution for the control variables would result in the distortion rather than the solution for the switching

mode (Debati e al.,2012). Therefore, it is the key to analyze IGBT on-off at the time of zero-crossing point and the dynamic operation of inductive current. Figure 8 displays the zero-crossing waveform as grid-connected current is ahead of the grid voltage, including grid-connected current waveform, grid voltage waveform, driving waveform of switch tube S_3, command current waveform and deadbeat control signal waveform. The corresponding waveform is appropriately adjusted for observation. Figure 8 (a) shows the waveform of each signal, and Figure 8 (b) displays the partial enlargement of zero-crossing point.

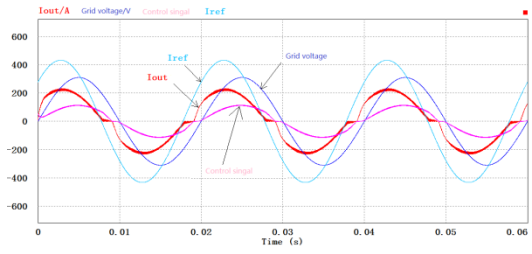

(a) Waveform diagram of grid-connected work as current lead

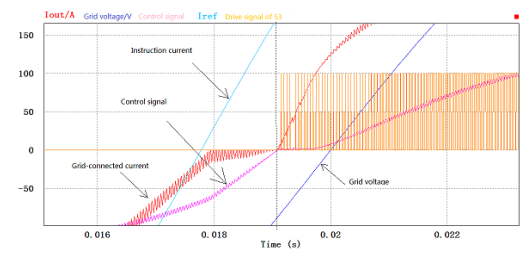

(b) Partial enlarged waveform diagram of zero-crossing point

Figure.9 Grid operating waveform of the current leading of unipolar modulation

The deadbeat control variable signal K, namely, the modulation signal in the unipolar modulation, is obtained by Equation (6). As K>0, S_1 is in an on-state, and S_3 is in a high-frequency on-off state. On the contrary, as K<0, S_2 is in an on-state, and S_4 is in a high-frequency on-off state. During the working process, K is determined by the command current signal, grid-connected current feedback signal and grid voltage feedback signal. Between the zero-crossing point of command current and the zero-crossing point of grid voltage, the grid-connected current is divided into two states by modulation signal K, that is, the trickle state between 0.018s and 0.019s, as well as the monotonic increasing state between 0.019s and 0.02s.

1. Trickle state

The command current is in the positive half-wave, and the grid voltage is in the negative half-wave with a greater value between 0.018 and 0.019s. Simultaneously, the modulating signal K obtained from Equation (6) is in the negative half-wave. Namely, the switch tube S_2 is on-state, and S_4 is in the high-frequency on-off state. As S_4 is in an on-state, the grid-connected current flows through U_{dc}+, S_2, L_4, grid E+, grid E-, L_3, S_4 and U_{dc}-. Simultaneously, the capacitance in the DC side inputs the active current to the grid and makes the inductance L_3 and L_4 charged, thus the inductive current linearly increases to the negative direction. As S_4 is in an off-state, the grid-connected current flows through S_2, L_4, grid E+, grid E-, L_3, VD_1 and S_2. At this time, the inductances L_3 and L_4 input the active current to the grid, and thus the inductive current linearly decreases to the positive direction. Hence, the grid-connected current in an on-state increases or decreases only in the negative half-wave, which makes the inductive current fail in tracking the command current smoothly to the positive half-wave. Thus there would generate a trickle state with a negative polarity. The working state of inverter circuit is shown in Figure 9.

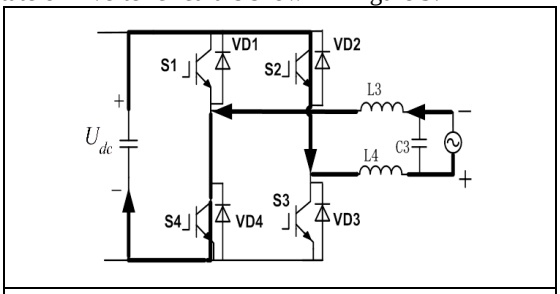

(a) S_2 is on-state, and S_4 is in on-state

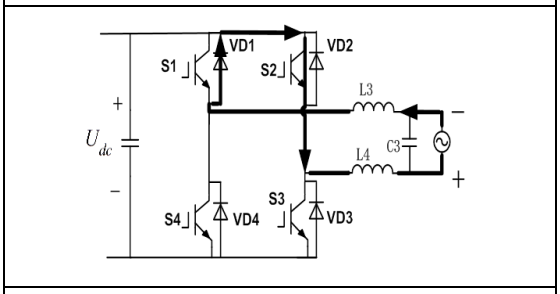

(b) S_2 is on-state, and S_4 is in the high-frequency off-state

Figure 10 The inverter circuit working state of trickle state state

2. Monotonic increasing state

With the gradual decrease of grid voltage to the positive direction, the modulation signal K turns to the positive polarity. So between 0.019s and 0.02s, the switch tube S_1 is on-state, and S_3 is in the high-frequency off-state. As S_3 is in an on-state, the grid-connected current flows through U_{dc}+, S_1, L_3, grid E+, grid E-, L_4, S_3 and U_{dc}-. Simultaneously, both the capacitance and grid in the DC side input the electricity to L_3 and L_4, as well as the inductive current increases to the positive direction with a larger slope. As S_3 is in an off-state, the grid-

connected current flows through S_1, L_3, grid E+, grid E-, L_4, VD_2 and S_1. At this time, the grid still input the electricity to the inductances L_3 and L_4, and the inductive current increases to the positive direction with a smaller slope. The working state of inverter circuit is shown in Figure 10.

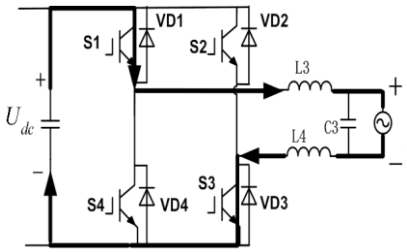

(a) S_1 is on-state, and S_3 is in on-state

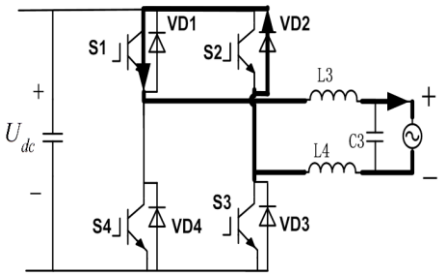

(b) S_1 is on-state, and S_3 is in the high-frequency off-state

Figure 11 The inverter circuit working state of monotonic increasing state

Hence, whether S_3 is in an on-state or in an off-state during the interval, the inductive current always has an on-state with a linear increase, thus resulting in the rapid increase in a short time. Likewise, the dynamic process from positive polarity to negative polarity of grid-connected current is similar to the analysis mentioned above. However, the difference is that S_1 and S_3 are in an on-state as well as S_2 and S_4 are in a monotonic increasing state.

Figure 11 presents the waveform as the grid-connected current lag behind the grid voltage. Moreover, there are still two working stages at zero-crossing point, namely, monotonic decreasing stage and slow rising stage.

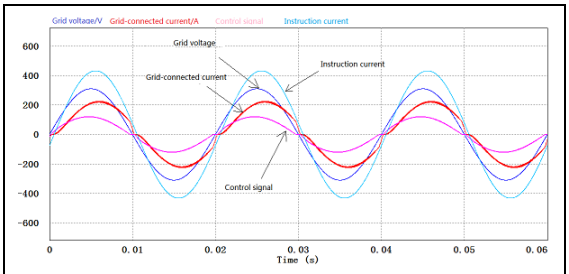

(a) Waveform diagram of grid-connected work as current lag

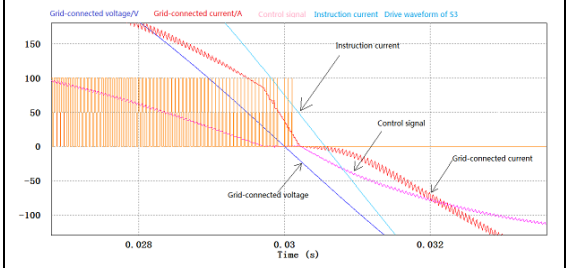

(b) Partial enlarged waveform diagram of zero-crossing point

Figure.12 Grid operating waveform of the current lagging of unipolar modulation

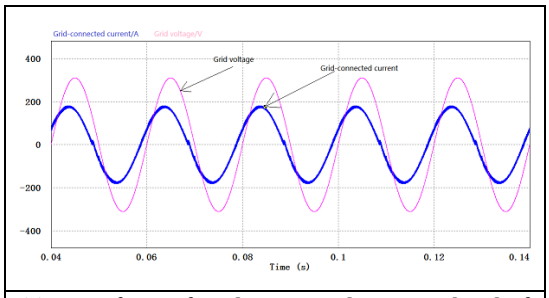

(a) Waveform of grid-connected current ahead of grid voltage

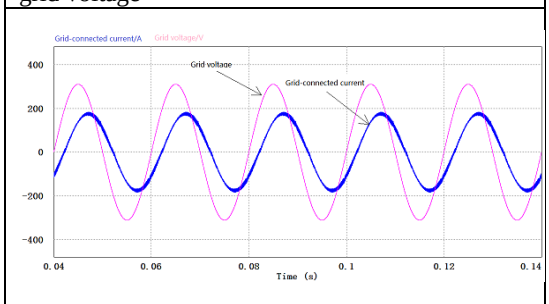

(b) Waveform of grid-connected current lagging behind grid voltage

Figure.13 Grid current and voltage waveform of the bipolar modulation

The lag of the command current makes its value higher around the zero-crossing point, and then the modulation signal decreases near zero point in advance, as well as the monotonic decreasing of grid-connected current starts. But the time for S_3 in an on-state is extremely short, almost zero. Then the grid-

connected current always flows along S_1, L_3, grid E+, grid E-, L_4, VD_2 and S_1. Furthermore, the inductance continues to discharge to input the active current to grid, hence, the inductance decreases along the negative direction with a larger slope.

When the modulation signal is less than zero, S_2 is in an on-state, and S_4 is in an on-off state with a small duty cycle. Simultaneously, the grid has increased to a larger value, which makes the inductive current increases to the negative direction with a slower rate.

Hence, the simple single-polarity modulation is no longer applicable in the photovoltaic grid-connected system with the reactive control. In addition, there is no distortion for the current at the zero-crossing point for the bipolar modulation, which is another advantage relative to unipolar modulation, except inhibiting common-mode current(Les et al.,2015). Figure 12 shows the grid-connected current waveform of bipolar modulation as reactive control. It is clearly seen that the bipolar modulation passes the zero point with a smooth transition and the grid-connected current waveform is ideal.

4 ANALYSIS FOR HYBRID MODULATION STRATEGY

UNIPOLAR modulation has significant advantages in harmonic, ripple and efficiency, however, the bipolar modulation has excellent properties on the grid-connected current control. Therefore, it is of great significance for cooperative control between photovoltaic grid connection and active power filter to study a kind of modulation mode with both advantages.

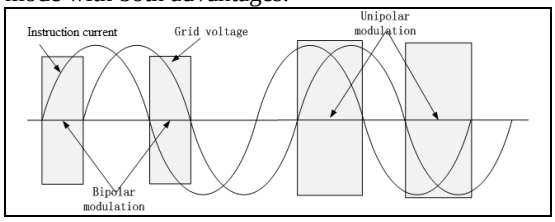

Figure.14 Schematic of Hybrid modulation principle

It is easily observed from the waveform of zero-crossing distortion by the unipolar modulation that the grid-connected current can be stably controlled when the polarity of instruction current is the same as that of the grid voltage. However, the polarity of instruction current is the opposite of that of grid voltage, the grid-connected current is out of control and produces distortion. Hence, the hybrid modulation mode of unipolar modulation in combination with the bipolar modulation was introduced. When the polarity of instruction current was the same as that of the grid voltage, the unipolar modulation was used as well as the advantages of unipolar modulation, such as small harmonic, low ripple and high efficiency, were fully utilized. When the polarity of instruction current is the opposite of that of grid voltage, the bipolar modulation was used to make the current realize the smooth transition of zero-crossing point as the system implemented reactive power control (Xu et al., 2008; Yan et al.,2010; Wang et al.,2016). Figure 13 shows the modulation mode principle based on this idea, and two kinds of modulation modes used the deadbeat algorithm for the modulating signal.

Therefore, the main circuit simulation model in Figure 5 should still be adopted, moreover, the judgement for polarities of command current and grid voltage is added, and then the simulation results are shown in Figure 14.

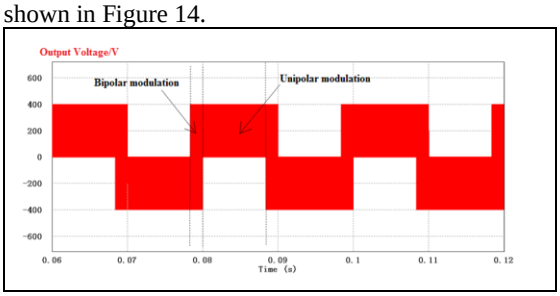

Figure 15 The output voltage waveform of grid-connected inverter by Hybrid modulation

Obviously, the output voltage of inverter has both the bipolar modulation and unipolar modulation in a grid period. Figure 15 shows the grid-connected current waveforms as ahead of, lagging behind, and synchronizing with the grid voltage. The grid-connected current waveform of hybrid modulation has small ripple as unipolar modulation and smooth transition as passing zero point as bipolar modulation.

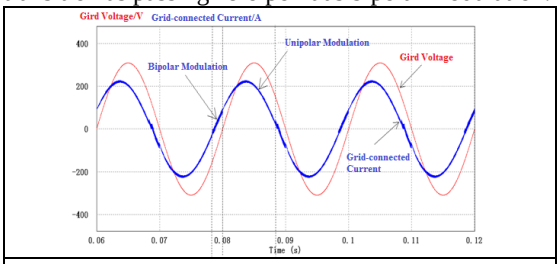

(a) the grid-connected current waveform ahead of the grid voltage.

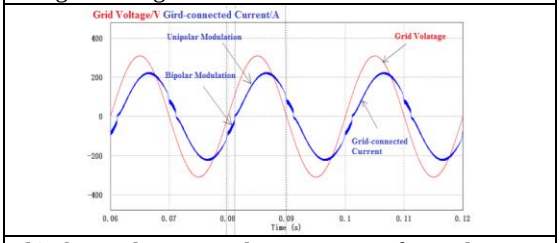

(b) the grid-connected current waveforms lagging behind the grid voltage.

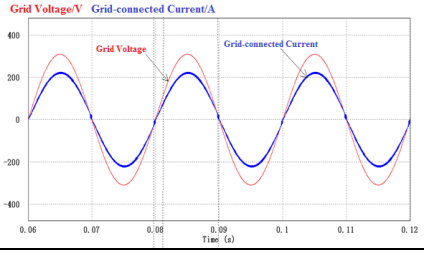

(c) the grid-connected current waveforms synchronizing with the grid voltage.

Figure 16 The current waveform of grid-connected inverter by Hybrid modulation

Figure 16 presents the spectrograms of three kinds of modulation ways with the same angle ahead of the grid voltage.

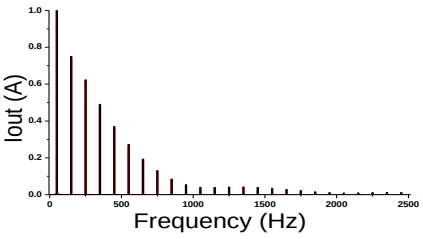

(a) the spcetrogram of unipolar modulation

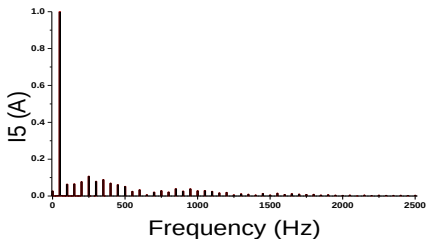

(b) the spcetrogram of bipolar modulation

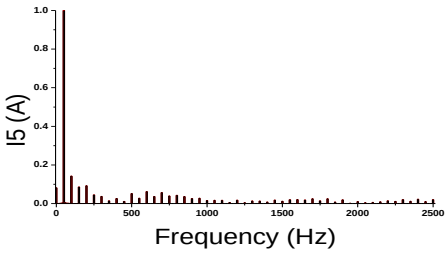

(c) the spcetrogram of hybrid modulation

Figure 17 The spectrograms of three kinds of modulation ways with the same angle ahead of the grid voltage

As the unipolar modulation, bipolar modulation and hybrid modulation are in the reactive control, the total harmonic distortion rates of grid-connected current are 8.47%, 4.82%, and 3.26%, respectively. Therefore, the unipolar modulation works for the hybrid modulation with the unit power factor output, which has all the advantages of unipolar modulation. As for the reactive control, the bipolar modulation plays an auxiliary role for control before the grid voltage passes the zero point. This can furthest ensure that the grid-connected inverter transports high-quality electrical energy as well as provide a reliable and efficient control method for photovoltaic grid-connected and collaborative control of active filtering.

5 EXPERIMENTAL RESULTS

THIS paper took a kind of 3 kW single-phase non-isolated photovoltaic grid-connected inverter as the experiment platform, and the topological structure was full-bridge inversion. When working under the full load of 3 kW, the phase ahead of or lagging behind the grid voltage for the output current of grid-connected inverter was controlled by the modes of unipolar modulation, bipolar modulation and hybrid modulation, as well as the power factor was adjusted around ±0.95. Finally, the test results were as follows.

As shown in Figure 17, zero-crossing distortion of current under the unipolar modulation are consistent with the results of the analysis. The total harmonic distortion rate of the grid-connected current was 9.824%.

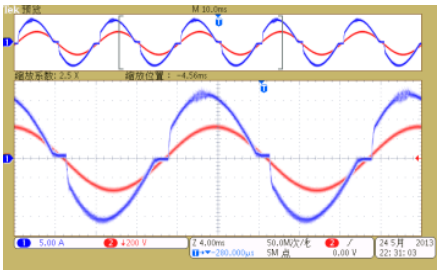

(a) Waveform of grid-connected current ahead of grid voltage

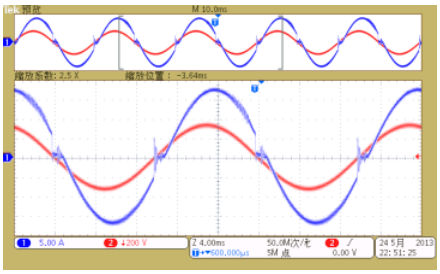

(b) Waveform of grid-connected current lagging behind grid voltage

Figure.18 Gird current waveform of the unipolar modulation

It is observed in Figure 18 that the grid-connected current under the bipolar modulation smoothly transited around the zero-crossing point of grid voltage. There was no distortion and the total harmonic distortion rate of the grid-connected current was 3.5%.

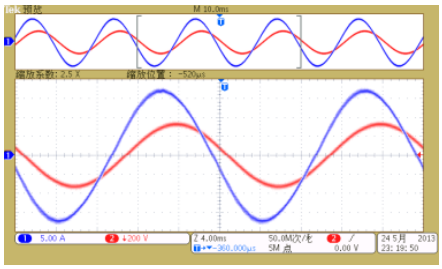

(a) Waveform of grid-connected current ahead of grid voltage

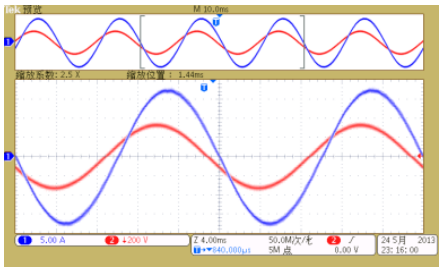

(b) Waveform of grid-connected current lagging behind grid voltage

Figure.19 Gird current waveform of the bipolar modulation

It is observed in Figure 19 that the grid-connected current under the hybrid modulation smoothly transited around the zero-crossing point of grid voltage. There was no distortion and the total harmonic distortion rate of the grid-connected current was 2.5%.

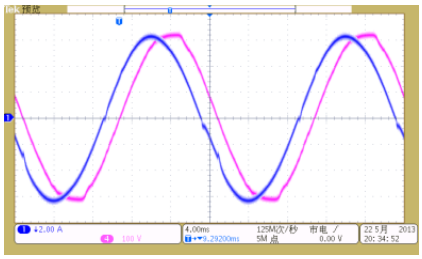

(a) Waveform of grid-connected current ahead of grid voltage

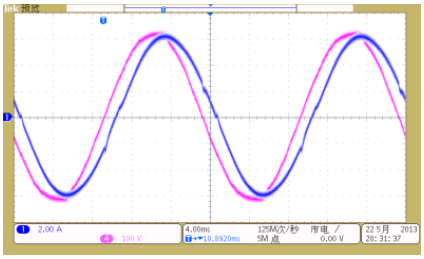

(b) Waveform of grid-connected current lagging behind grid voltage

Figure.20 Gird current waveform of the Hybrid modulation

The above test results showed that the total harmonic distortion rates of the grid-connected current were 9.824% by unipolar modulation, 2.5% by bipolar modulation and 3.5%, respectively, by the hybrid modulation as the reactive power control by three kinds of modulation modes. Thus, the hybrid modulation can transform into the unipolar modulation for control and had all the advantages of the unipolar modulation as the output of unit power factor. Moreover, as the reactive power control, the bipolar modulation as the auxiliary control was introduced around the zero-crossing point of grid voltage. This can furthest ensure that the high-quality electric energy can be transported to the power grid by the grid-connected inverter, thus providing a reliable and high-efficiency control method for the photovoltaic grid connection.

6 REFERENCES

Baifeng Chen, Pengwei Sun, Chuang Liu. High Efficiency Transformerless Photovoltaic Inverter with Wide-Range Power Factor Capability [J]. IEEE Trans. Power Electron, 2008,23(3): 1320-1333.

Debati Marandi, Tontepu Naga Sowmya, B Chitti Badu. Comparative Study between Unipolar and Bipolar Switching Scheme with LCL Filter for Single-Phase Grid Connected Inverter System [J]. IEEE Students' Conference on Electrical, Electronices and Computer Science, 2012:1659-1665.

Kjaer S B, Pedersen J K, Blaabjerg F.A Review of Single-Phase Grid-Connected Inverters for Photovoltaic Modules[J]. IEEE Trans. On Industry Applications, 2005, 41(5):1292-1306.

Lasseter R H. Microgrids and Distributed Generation[J]. Intelligent Automation & Soft Computing, 2010, 16(2):225-234.

Les Bowtell, Tony hfock. Comparison Between Unipolar and Bipolar Single Phase Grid-Connected Inverters for PV Applications[J]. IEEE Transactions on Industry Applications, 2015, 41(5):1292-1306.

Li Hong, Fang Chunxue, Hao Ruixiang, et al. Harmonic generation mechanism and suppression method of grid-connected photovoltaic inverter with source clamp [J]. Chinese journal of electrical engineering, 2017, 37(23):6971-6980.

Liu Guohai, Cheng Ran, Zhao Wanxiang, et al. Improved direct torque control of five-phase permanent magnet motor considering third-order harmonic suppression [J]. Chinese journal of electrical engineering, 2017, 37(14):4212-4221.

Ma Qizhi, Xie Xuqin, Deng Zhuohui, et al. Research on railway harmonic suppression based on high-pass filter [J]. Journal of electrical engineering, 2017, 12(2):1-7.

Manjili Y S, Vega R, Jamshidi M. Cost-Efficient Environmentally-Friendly Control of Micro-Grids Using Intelligent Decision-Making for

Storage Energy Management[J]. Intelligent Automation & Soft Computing, 2013, 19(4):22.

Wang Fusheng, Zhang Dehui, Dai Zhiqiang, et al. Hybrid modulation strategy of cascade h-bridge photovoltaic grid-connected inverter [J]. Journal of electrical technology, 2016, 31(A01):137-145.

Wang Guofeng, Wang Guoqing, Zhang Hongtao, el ta. Research on a Novel Single-phase Non-isolated PV Grid-connected Inverter [J]. Power Electronics: 2013,47(3):45-47.

Wang Jidong, Li Hongan, Li Guodong, etc. Comprehensive Configuration Method to Suppress Harmonics in Active Distribution Network[J]. Proceeding of the CSU-EPSA, 2017,29(4):13-19.

Xiao Huafeng, Liu Xipu, Lan Ke. Non-isolated pv grid-connected inverter with zero-voltage conversion H6 structure [J]. Chinese journal of electrical engineering, 2014, 34(3):363-370.

Xie Ning, Luo An, Ma Fujun, et al. Harmonic Interaction Between Large-scale Photovoltaic Power Stations and Grid[J].Proceedings of the CSEE, 2013,33(34):9-16.

Xu Zheng, Wang Hui, Li Youchun. A Hybrid Modulation Scheme for Grid-connected Photovoltaic Systems[J]. Electric Utility Deregulation and Restructuring and Power Technologies, 2008, 1109(10):2707-2711.

Yan Chaoyang, Jia Minli, Zhang Chunjiang, et al. Principle and implementation of HPWM modulation strategy for three-phase high-frequency chain matrix inverter [J]. Journal of electrical technology, 2010, 25(11):113-121.

Yi Lingzhi, Liu Zhongfan, Chen Caixue, etc. A New Non-isolated Single-phase Photovoltaic Grid-connected Inverter with H6-type Configuration[J]. Journal of Power Supply: 2015,49(6):80-82.

Yuan Yisheng, Zhang Weiping, Zhu Benyu, et al. Topology and common mode current analysis of a novel non-isolated photovoltaic grid-connected inverter [J]. Power grid technology, 2014, 38(12):3286-3292.

Zhao Yong, Yang Zilong, Cao Dufeng, et al. Harmonic analysis and suppression of junction points of photovoltaic power stations in weak power grid [J]. Acta solarica sinica, 2018(1):117-123.

Zhu Guofeng, Mu Longhua. Optimal Control of Distributed Harmonic Compensation in Low-Voltage Distribution Network with Multiple Feeders[J]. Transactions of China Electrotechnical Society, 2016,31(9):25-33.

7 NOTES ON CONTRIBUTOR

Liao Tian-fa, doctor, associate professor, main research direction: power electronics and special power supply, etc.
E-mail: liaotianfa@163.com